Papanoa, Mexico earthquake of 18 April 2014 (M_w7.3)

UNAM Seismology Group
(with contribution from Universidad Autónoma Metropolitana, Azcapotzalco, Mexico D.F.)

Resumen

El sismo de Papanoa rompió la interfase de la placa al noroeste de la brecha sísmica de Guerrero. En esta región, los grandes sismos anteriores ocurrieron en 1943 (M_S 7.4), 1979 (M_w7.4) y 1985 (M_w7.5). El terremoto se registró en la región cercana a la fuente por varios acelerógrafos. Daño severo se reportó en Papanoa (donde *PGA* regisrado en una de las componentes horizontales en un sitio blando fue de ~ 0.9 g) y otras ciudades costeras cercanas. También se sintió con fuerza en la Ciudad de México, donde los movimientos de tierra fueron comparables a los registrados durante los sismos de 1979 y de 1985.

Con un análisis cuidadoso de datos cercanos a la fuente, incluyendo la polarización de la onda *P*, se obtiene un epicentro en 17.375 ºN, 101.055 ºW, cerca de la costa y de la localidad de Papanoa. La duración efectiva del movimiento del suelo en las estaciones costeras cercanas a la fuente, al NW del epicentro, es 10 a 15 s, mientras que es de 20 a 35 s en las estaciones del SE, lo que demuestra la directividad de la ruptura hacia Zihuatanejo. Tres (en algunos casos sólo dos) emisiones de radiación de alta frecuencia son visibles en los acelerogramas. Los registros de campo cercano muestran que el deslizamiento fue pequeño durante los primeros 2-3 s de la ruptura que, posteriormente, fue seguido de dos o tres subeventos más grandes en cascada. La inversión del deslizamiento a partir de ondas de telesísmicas, junto con los datos GPS de un par de sitios cercanos a la fuente, revela que la ruptura consistió principalmente de dos subeventos. El primero estuvo centrado cerca del hipocentro y tuvo un radio de ~ 15 km. El segundo evento, más o menos de la misma dimensión que el primero, se centró ~ 25 km al SSE de Zihuatanejo. Un análisis previo de tres eventos de deslizamiento lento (SSE) en la región (2001-2002; 2006; 2009-2010) había revelado que esta región tiene un acoplamiento alto (> 0.5) en el período inter-SSE, con un déficit de deslizamiento cerca de cuatro veces mayor que en la brecha sísmica NW de Guerrero (Radiguet *et al*., 2012). Parece que el deslizamiento grande correspondiente al primer subevento del sismo de 2014 experimentó un deslizamiento acumulado de ~ 20 cm durante los SSE, lo que sugiere que el deslizamiento sísmico y los SSE pueden compartir la misma zona de la interfase. Alternativamente, el deslizamiento durante el SSE puede haber ocurrido en un área que rodea la region del deslizamiento grande, lo que parece un modelo físicamente más plausible.

Los epicentros de las réplicas ($M \geq 3.5$), que se produjeron en las próximas 36 horas, definen un área rectangular de ~ 40 km × 70 km, orientada ~ N75ºE; cerca de la mitad de esta región se encuentra en tierra. Esta zona encierra la región de deslizamiento obtenida en la inversión. Más de la mitad de la zona de réplicas se sobrepone con la del sismo de 1979 y una pequeña fracción con la del sismo 21 de septiembre 1985. Como sólo conocemos la distribución del deslizamiento del sismo de 2014, no se sabe si las dos regiones de gran deslizamiento también se deslizaron de

Instituto de Ingeniería
Universidad Nacional Autónoma de México
Circuito de la Investigación Científica s/n
Ciudad Universitaria
Delegación Coyoacán, 04510
México D.F. México

Departamento de Sismología
Instituto de Geofísica
Universidad Nacional Autónoma de México
Circuito de la Investigación Científica s/n
Ciudad Universitaria
Delegación Coyoacán, 04510
México D.F. México
Corresponding autor: krishnamex@yahoo.com

Instituto de Geofísica
Universidad Nacional Autónoma de México
Circuito de la Investigación Científica s/n
Ciudad Universitaria
Delegación Coyoacán, 04510
México D.F. México

Servicio Sismológico Nacional
Universidad Nacional Autónoma de México
Circuito de la Investigación Científica s/n
Ciudad Universitaria
Delegación Coyoacán, 04510
México D.F. México

manera similar durante los sismos anteriores. El sismo fue seguido por dos sismos moderadamente grandes que se produjeron el 8 de mayo (M_w6.5) y 10 de mayo (M_w6.1). Los epicentros de estos eventos caen cerca de Tecpan, dentro de la brecha sísmica NW de Guerrero (que se extiende de 100 ºW a 101 ºW), fuera de la zona de réplicas del sismo de Papanoa. No ha ocurrido un gran sismo en esta zona de la brecha, entre Papanoa y Acapulco, desde los acontecimientos de 1899 (M_s7.5) y 1911 (M_s7.6). Sin embargo, la sismicidad en la región (en niveles de $M_w \geq$ 5) parece normal. Se han identificado pocos sismos moderados de duración inusualmente grande y con radiación de alta frecuencia deficiente cerca de la trinchera. En contraste con la region de Papanoa - Zihuatanejo, en este segmento se tiene un acoplamiento inter-SSE, desde unos 10 km al interior hacia el mar, muy bajo (< 0.2) y el déficit de deslizamiento es aproximadamente una cuarta parte del de la región Papanoa- Zihuatanejo (Radiguet *et al*., 2012). Como consecuencia, el período de recurrencia esperado de grandes sismos puede ser relativamente largo, de acuerdo con la sismicidad de la región Papanoa-Acapulco.

Palabras clave: sismo de Papanoa, movimientos fuerte, evento de deslizamiento lento, brehas sísmica de Guerrero.

Abstract

Papanoa earthquake broke the plate interface NW of the Guerrero seismic gap. In this region, previous large earthquakes occurred in 1943 (M_s 7.4), 1979 (M_w7.4) and 1985 (M_w7.5). The earthquake was recorded in the near-source region by several accelerographs. Severe damage was reported in Papanoa (where *PGA* of ~ 0.9 g was recorded on one of the horizontal components at a soft site) and other nearby coastal towns. It was also felt strongly in Mexico City where the ground motions were comparable to those recorded during the 1979 and 1985 events.

A careful analysis of the near-source data, including *P*-wave polarization, yields an epicenter at 17.375 ºN, 101.055 ºW, close to the coast, near the town of Papanoa. Effective duration of ground motion at near-source coastal stations to the NW of the epicenter is 10-15 s, while it is 20-35 s to the SE, demonstrating rupture directivity towards Zihuatanejo. Three (in some cases only two) bursts of high-frequency radiation are visible in the accelerograms. Near-field records show that the slip was small during the initial 2-3 s of rupture which, subsequently, cascaded in two or three larger subevents. Slip inversion using teleseismic waves, along with GPS data from a couple of near-source sites, reveals that the rupture mainly consisted of two subevents. The first one was centered close to the hypocenter and had a radius of ~ 15 km. The second subevent, roughly of the same dimension as the first, was centered ~ 25 km SSE of Zihuatanejo. Previous analysis of three slow slip events (SSEs) in the region (2001-2002; 2006; 2009-2010) had revealed that this region had a high inter-SSE coupling ratio (> 0.5) with a slip deficit about four times greater than in the adjacent NW Guerrero seismic gap (Radiguet *et al*., 2012). It seems that the large slip patch corresponding to the first subevent of the 2014 earthquake experienced a cumulative slip of ~ 20 cm during the SSEs, suggesting that seismic and SSE slip may share the same area of the interface. Alternatively, the SSE slip may have occurred over an area surrounding the large slip patch, a physically more plausible model.

Epicenters of aftershocks ($M \geq 3.5$), which occurred in the next 36 hours, define a rectangular area of ~ 40 km × 70 km, oriented ~ N75ºE; about half of this area lies onshore. This area encloses the inverted slip region. More than half of the aftershock area overlaps with that of the 1979 earthquake and a small fraction with that of the 21 September 1985 earthquake. As we only know the slip distribution of the 2014 earthquake, it is not known if the two large-slip patches had also slipped similarly during the previous earthquakes.

The earthquake was followed by two moderately large events that occurred on 8 May (M_w6.5) and 10 May (M_w6.1). The epicenters of these events fall near Tecpan, within the NW Guerrero seismic gap (which extends from 100 ºW to 101 ºW), outside the aftershock area of the Papanoa earthquake. No large earthquake has occurred in this part of the gap, between Papanoa and Acapulco, since the events of 1899 (M_s7.5) and 1911 (M_s7.6). However, seismicity in the region (at $M_w \geq 5$ level) appears normal. A few moderate earthquakes of unusually large duration and deficient high-frequency radiation have been identified near the trench. In contrast to the Papanoa – Zihuatanejo region, in this segment the inter-SSE coupling ratio from ~ 10 km inland towards sea is very low (< 0.2) and the slip deficit is about one-fourth that of the Papanoa- Zihuatanejo region (Radiguet *et al*., 2012). As a consequence, the expected recurrence period of large/great earthquakes may be relatively long, in agreement with the seismicity of the Papanoa-Acapulco region.

Key words: Papanoa earthquake, strong motion, slow-slip event, seismic gap of Guerrero.

Introduction

Seismic activity was very intense along the Guerrero segment of the Mexican subduction zone between 1899 and 1909. During this period seven large/great earthquakes occurred on the plate interface between ∼ 99 ºW and 101 ºW [24 Jan. 1899, M_S7.5; 15 Apr. 1907, M_S7.7, M_w7.9; 26 Mar. 1908, M_S7.6, M_w7.5; 27 Mar. 1908, M_S7.0, M_w7.2; 30 Jul. 1909; M_S7.3, M_w7.5; 31 Jul. 1909, M_S6.9, M_w7.0; 16 Dec. 1911, M_S7.6, M_w7.6] (Figure 1) (Appendix A). Instrumental locations of these earthquakes are very poor. The damage and felt reports along the Guerrero coast of Mexico of some of these events are not extensive enough to delineate their rupture areas with confidence. The exceptions are the earthquakes of 1907 and 1909 whose rupture areas were near the towns of San Marcos (∼ 99.2 ºW) and Acapulco (∼ 100 ºW), respectively (Appendix A). Thus, there is little doubt that the plate interface near Acapulco and SE of it broke during some of the events of the 1899-1911 sequence. The damage reports also suggest, *albeit* less conclusively, that 1899 and 1911 earthquakes ruptured the interface NW of Acapulco between 100 ºW and 101 ºW.

The segment between ∼ 99 ºW and 100 ºW experienced large earthquakes on 11 May 1962 (M_S7.0, M_w7.2), 19 May 1962 (M_S6.7, M_w7.2), 28 Jul. 1957 (M_S7.5, M_w7.7), and 25 Apr. 1989 (M_w6.9) (Figure 1). However, no large earthquake ($M_w ≥ 7.0$) has occurred between 100 ºW and 101 ºW at least since 1911. Immediately to the NW of 101 ºW, the plate interface ruptured in 22 Feb. 1943 (M_S7.5, M_w7.4), 14 Mar. 1979 (M_w7.4), and 21 Sep. 1985 (M_w7.5) (Figure 1). Based on this seismic history, the segment from ∼ 99 ºW to 101 ºW was designated a seismic gap and was called the Guerrero seismic gap (Singh *et al*., 1981). The fact that the occurrence of large earthquakes is clearly documented between ∼ 99 ºW and 100 ºW but is uncertain between ∼ 100 ºW and 101 ºW, it is convenient to divided the gap in two segments: the NW segment extending from ∼ 100 ºW to 101°W, henceforth called the NW Guerrero gap, and the SE segment from 99 ºW to 100 ºW, henceforth denoted as the SE Guerrero gap (Ortiz *et al*., 2000). Since recurrence period of large earthquakes along the Mexican subduction zone is about 30 to 60 years (Singh *et al*., 1981), the SE Guerrero region may also be considered a mature seismic gap.

Anticipation of large/great earthquakes in the region led to the installation of Guerrero Accelerographic Array in 1985 (Anderson *et al*., 1986, 1994). Soon after the completion of the array, the Michoacán earthquakes of 19 and 21 September1985 (M_w8.0, 7.5) ruptured the plate interface NW of the seismic gap. The earthquake of 19 September 1985 caused unprecedented damage and death in Mexico City, which led to increased concern about the occurrence of similar earthquakes in Guerrero. As a consequence, the accelerographic and seismic networks in the region were improved and strengthened, and a seismic alert system for Mexico City, triggered by earthquakes in the gap, became operational. A seismic network was operated during 1987-1993 to monitor the seismicity and to map the geometry of the subducted Cocos plate beneath the region (Suárez *et al*., 1990). In a collaborative effort among Caltech, U.C. Los Angeles and UNAM, called the MesoAmerican Subduction Experiment (MASE), a portable array of 100 broadband seismographs, spaced 5 km apart, was operated between Acapulco and Tampico during 2005-2007 (Pérez-Campos *et al*., 2008). Analysis of the data produced by the permanent networks, and temporary and portable arrays has resulted in a much improved knowledge of seismicity and seismotectonics of the region, including the geometry of the subducted Cocos plate (e.g., Suárez *et al*., 1990; Singh and Pardo, 1993; Pardo and Suárez, 1995; Pérez-Campos *et al*., 2008; Song *et al*., 2009; Husker and Davis, 2009; Pacheco and Singh, 2010). Seismicity and focal mechanisms in the Guerrero segment, based on local and regional data, reveal that the Cocos plate subducts below Mexico at a shallow angle, reaching a depth of 25 km at a distance of 65 km from the trench (∼ 5-10 km inland from the coast). An unbending of the slab begins at this distance. The slab becomes horizontal at a distance of ∼ 120 km at a depth of 40 km. Earthquakes and focal mechanisms shown in Figure 1b, based on Table 1 of Pacheco and Singh (2010), summarizes the seismicity and seismotectonics of the region: (a) a relatively wide band (∼ 60-65 km) of shallow–dipping thrust events which extends from near the trench up to the coast, (b) a narrow band of events about 15-25 km inland in the depth range of 25-40 km, mostly exhibiting downdip compression, (c) a hiatus in the inslab seismicity from about 85 to 160 km from the trench and a resumption of normal-faulting earthquakes which, finally, cease at a distance of ∼ 240 km. There is also evidence of a thin (∼ 3-5 km) ultraslow velocity, high-pore pressure fluid layer at the top of the subducted oceanic crust of the slab (Song *et al*., 2009; Kim *et al*., 2010).
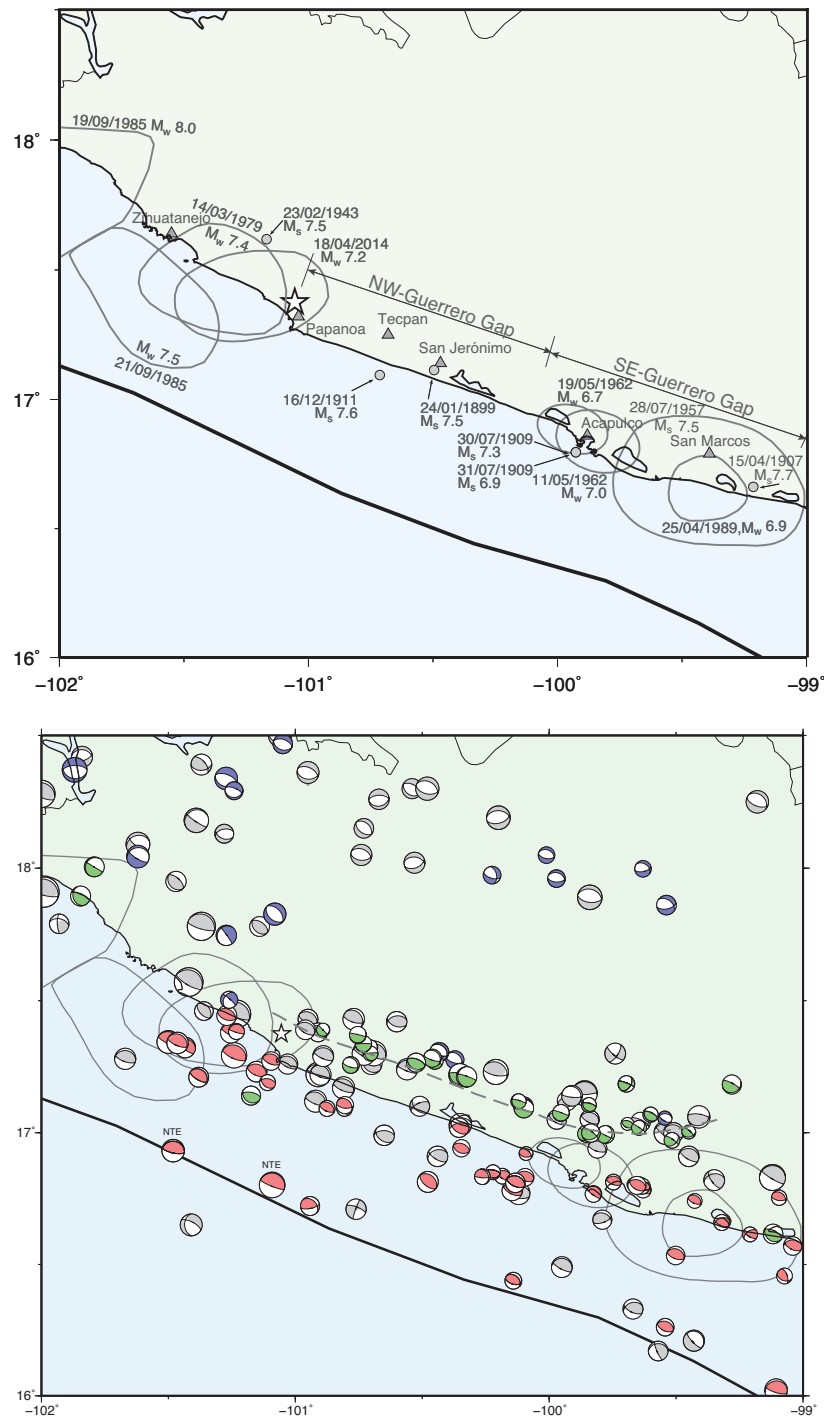
Figure 1. (a) Tectonic setting and epicenter or estimated rupture areas of large earthquakes in and near Guerrero segment of the Mexican subduction zone. The epicenters of 1899-1911 earthquakes have large uncertainty (Appendix A). Earthquakes of 1908 fall outside the area covered by the map. Lack of large earthquakes since at least 1911 between ~100 ºW – 101 ºW defines the NW Guerrero seismic gap. Except for the doublet of 1962 (MS7.1, 7.1) and the earthquake of 1989 (Mw6.9), no large/great event has occurred inthe segment between ~99 ºW – 100 ºW since 1957. This segment is designated as the SE Guerrero seismic gap. (b) Focal mechanisms of well-located earthquakes using local and regional data (adopted from Pacheco and Singh, 2010) are shown at their epicenters in red (shallow-dipping thrust), green (steeply-dipping thrust), and blue (normal fault). Epicenters and mechanisms of earthquakes in grey are taken from global CMT catalog; the locations of these events are not well determined from local and regional data. Dashed green line defines the transition between shallow-dipping interplate and steeply-dipping intraslab earthquakes. NTE: near-trench earthquakes with deficient high-frequency radiation and large centroid delay time.

Table 1. Source parameters of the 18 April 2014, Papanoa, Mexico earthquake.

Source	Lat., °N	Lon., °W	Depth, km	Strike, °	Dip, °	Rake, °	M_0, Nm
This study	17.375	101.055	15[*]	-	-	-	-
SSN	17.182	101.195	18.0	-	-	-	-
Regional *W*-phase[+]	17.35	101.230	21.5	300	23	95	8.58×10^{19}
NEIC	17.397	100.972	10	-	-	-	-
USGS, CMT	17.397	100.972	10	312	23	114	7.72×10^{19}
USGS, *W*-phase, CMT	17.397	100.972	21.5	302	20	99	8.49×10^{19}
Global CMT	17.55	101.25	18.9	303	18	98	1.00×10^{20}

[*] Depth fixed.
[+] Based on a real-time algorithm implemented at Institute of Geophysics, UNAM, which uses regional waveforms recorded on SSN broadband stations. The depth was fixed in the inversion and a grid search was performed for the centroid location.

The region is also equipped with a sparse distribution of continuous GPS stations. This network has detected the occurrence of large, slow seismic events (SSEs) in the region with a periodicity of ~ 4 years: in 1997-1998, 2001-2002, 2006, and 2009-2010 (e.g., Lowry *et al*., 2001; Kostoglodov *et al*., 2003; Iglesias *et al*., 2004; Yoshioka *et al*., 2004; Kostoglodov *et al*., 2010; Radiguet *et al*., 2011; Radiguet *et al*., 2012). In these episodes the slow slip in NW Guerrero was not only confined to the near-horizontal segment of the plate interface but extended to the updip portion of the slab up to ~ 10 km inland from the coast, at least for the 2006 event (Radiguet *et al*., 2011; Cavalié *et al*., 2013). The source inversion shows that part of the slip area may have extended offshore. Radiguet *et al*. (2012) and Cavalié *et al*. (2013) report that, due to such aseismic energy release, the secular slip deficit in the seismogenic zone of the NW Guerrero seismic gap is one fourth of the adjacent segments, suggesting that this may be the reason for longer recurrence period in the segment. The most recent SSE in the region began in January, 2014. The 18 April 2014 Papanoa earthquake (M_w7.3) occurred during this SSE episode.

In the context of the SSEs and other related phenomena (e.g., tectonic tremors) observed in the region, and the concern over the seismic potential of the Guerrero seismic gap, a detailed study of the Papanoa earthquake acquires special interest. In this paper, we present an analysis of the earthquake and the subsequent seismic activity in the region based, mostly but not exclusively, on local and regional data.

Earthquake of 18 April 2014

Local recordings and the location of the earthquake

In and near the epicentral region, there were two permanent broadband stations (ZIIG and CAIG) belonging to Servicio Sismológico Nacional (SSN, Mexican Seismological Service), which are also equipped with accelerometers and GPS receivers, and four accelerographic stationsbelonging to the Institute of Engineering, UNAM (PET2, SLU2, NUX2, and SUCH) (Figure 2). In addition, there were four accelerographic stations (GR01, GR02, GR13, GR14), belonging to the Mexican seismic alert system (SASMEX), which recorded the event. SASMEX data could not be used in location and in quantitative analyses since these accelerograms did not have absolute time and the quality of recordings was relatively poor. The broadband seismograms at ZIIG and CAIG were clipped during the mainshock. We used accelerograms at these stations in our analysis.

The location of the earthquake presented usual problems associated with large coastal earthquakes in Mexico. It was difficult to pick *S* wave corresponding to the first *P* wave on local recordings. The density of stations is

Figure 2. Permanent stations in the epicentral region. Azimuths of the hypocenter of the mainshock with respect to stations ZIIG, PET2, SLU2, SUCH, and NUX2, determined from P-wave polarization, are shown. The location of the mainshock and the aftershocks 8 May (Mw6.5) and 10 May (Mw6.1) are shown by circles and are marked M, A1, and A2, respectively.

still relatively sparse and crustal structure too poorly known for precise location of the event with only the arrival times of *P*-wave. *P*-waves of this earthquake on local seismograms were emergent. Thus, to locate the earthquake we used both *P*-wave arrival time and azimuth of the source at stations ZIIG, PET2, SLU2, NUX2, and SUCH (Figure 2). We measured the azimuth by plotting the horizontal displacement polarization during the first 3 s of *P* wave (Figure 3). The convergence of the azimuths points to a source near the town of Papanoa (Figure2). We fixed the depth at 15 km and searched for a location in the neighborhood of the convergence area which, using the crustal model employed by SSN, gave the minimum *P*-wave arrival-time *rms* error. This location is given in Table 1 along with those reported by other agencies. We note that the GCMT epicenter is 28 km to N47ºW of the epicenter obtained from local data (Figure 2).

Some observations from local recordings

Figure 4 shows plots of acceleration, velocity, and displacement traces at local stations from NW of the epicenter (UNIO, ZIIG, PET2) to the SE (SLU2, NUX2, SUCH, CAIG). The velocity and displacement traces were obtained from direct integration of the accelerograms. The traces begin at the arrival of *P* wave. As expected, the static displacements at most stations are unreliable. This is illustrated in Figure 5 where the displacements at ZIIG from double integration of acceleration traces and

1-s GPS data are compared (GPS station ZIHU is collocated with the seismographic station ZIIG). The figure demonstrates the need for collocation of accelerograph and GPS receiver if we wish to retrieve true ground displacement valid from infinite period to high frequencies. The static displacement at Tecpan GPS site was negligible as was also the case at CAIG.

Figure 4 includes plots of $I_i(t) = \int a_i^2(t)dt$, where the integration is performed beginning at the arrival of P wave up to the end of the accelerogram, and i refers to the component of the accelerogram. The plots list the "effective" duration of each component, defined here as the time window that includes 5 to 95% of $I_i(t)$.

Some source characteristics can be inferred from the visual inspection and preliminary analysis of local recordings:

1. The effective durations on the horizontal components at UNIO, ZIIG, and PET2 (to the NW of epicenter) range between 10 to 15 s while it is between 20 to 35 s at SLU2, NUX2, SUCH, and CAIG (stations to the SE of the epicenter). This suggests that the rupture propagated towards NW. Negligible static displacement field at Tecpan shows that the rupture did not extend till this town.

2. Three bursts of high-frequency radiation are visible in the acceleration traces at SLU2, NUX2, and SUCH. Two bursts are also seen at PET2. At ZIIG and UNIO the two bursts are not very clear.
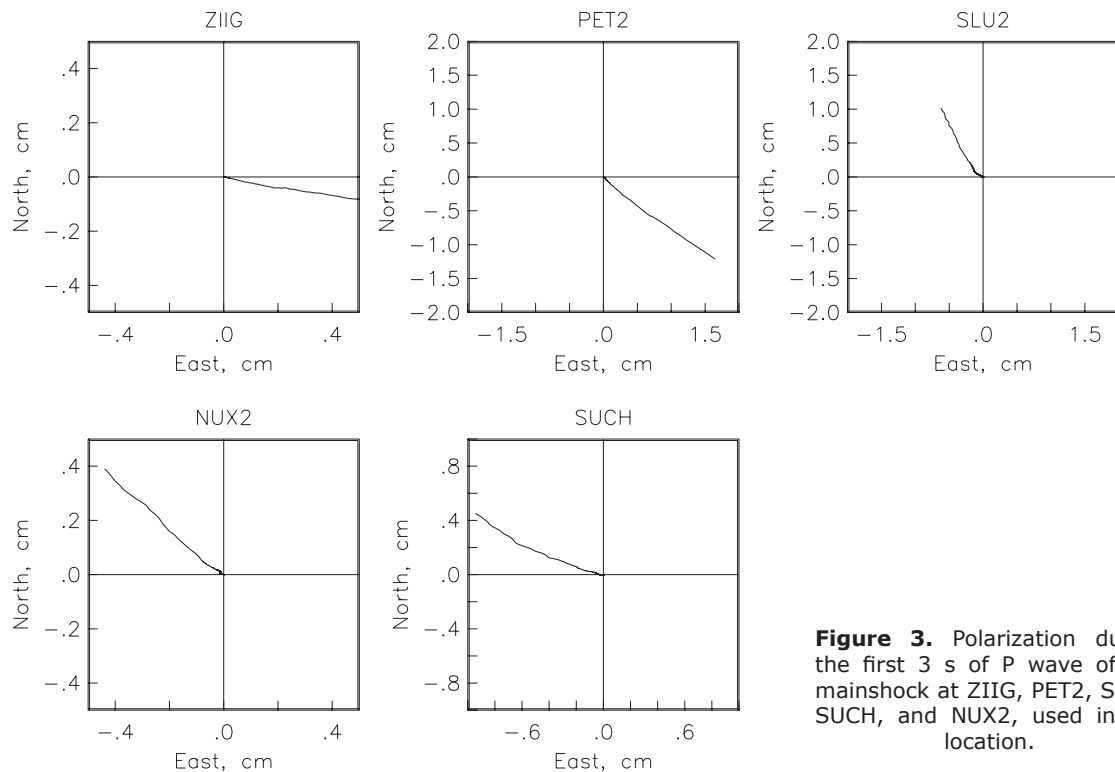
Figure 3. Polarization during the first 3 s of P wave of the mainshock at ZIIG, PET2, SLU2, SUCH, and NUX2, used in the location.

3. The displacement traces at SLU2, NUX2, and SUCH are dominated by a single, simple *S*-pulse. The displacements at these stations corresponding to the two later high-frequency bursts are relatively small. *S*-waves from the second and third bursts at these stations arrive ~ 7 s and 20 s after the *S* wave from the first burst. The displacement traces at PET2 and ZIIG consist of three, closely-spaced *S*-pulses. A simple working model, consistent with the observations, may consist of three sources, the first involving larger slip than the other two. The first source is located near the hypocenter ~ 20 km NW of SLU2,near the town of Papanoa (Figure 2). The second source is located roughly 10 km from the first source towards PET2. The third source is located between PET2 and ZIIG. Because of the proximity of the second and third sources, and larger slip during the first source, their corresponding *S* pulses are seen at PET2 and ZIIG. However, the latter two sources are relatively far from SLU2, NUX2, and SUCH. Hence, the first pulse dominates the record.

4. A subsidence of ~ 4 cm at ZIIG (Figure 5) suggests that if the rupture propagated up to this station then the slip on the fault probably did not extend more than about 8 km inland of this station. This conjecture is based on Okada's model (Okada, 1992; Figure 3 of Singh *et al*., 2012).

Slip on the fault from inversion of teleseismic seismograms with some constrain from local GPS data

Results from slip inversion, based on teleseismic data, were reported soon after the earthquake by NEIC and C. Mendoza (personal communication, 2014). NEIC inversion uses the NEIC hypocenter (17.6 °N, 100.7 °W, *H* = 24 km; Table 1). It shows two patches of slip: a compact, approximately circular area of ~10 km radius centered at the hypocenter and a diffused second patch with maximum slip occurring ~ 35 km to the WSW of the first patch. The moment rate function includes a third pulse which begins about 27 s after the first pulse and lasts for ~ 16 s. The slip distribution obtained by C. Mendoza, who uses 17.55 °N, 100.82 °W, *H* = 24 km as the hypocenter, is similar to that reported by NEIC. Since the locations used by NEIC and C. Mendoza are 45 km to N56ºE and 32 km to the N52ºE, respectively, with respect to the location estimated here, the slip areas obtained in these inversions are shifted inland accordingly.

In our inversion we applied the same simulated-annealing, wavelet domain wave-form inversion algorithm as used by NEIC (Ji *et al.*, 2002a, b) to invert teleseismic body and surface waves for the slip on the fault plane. We used a total of 29 *P*-waves, 34 *S*-waves,
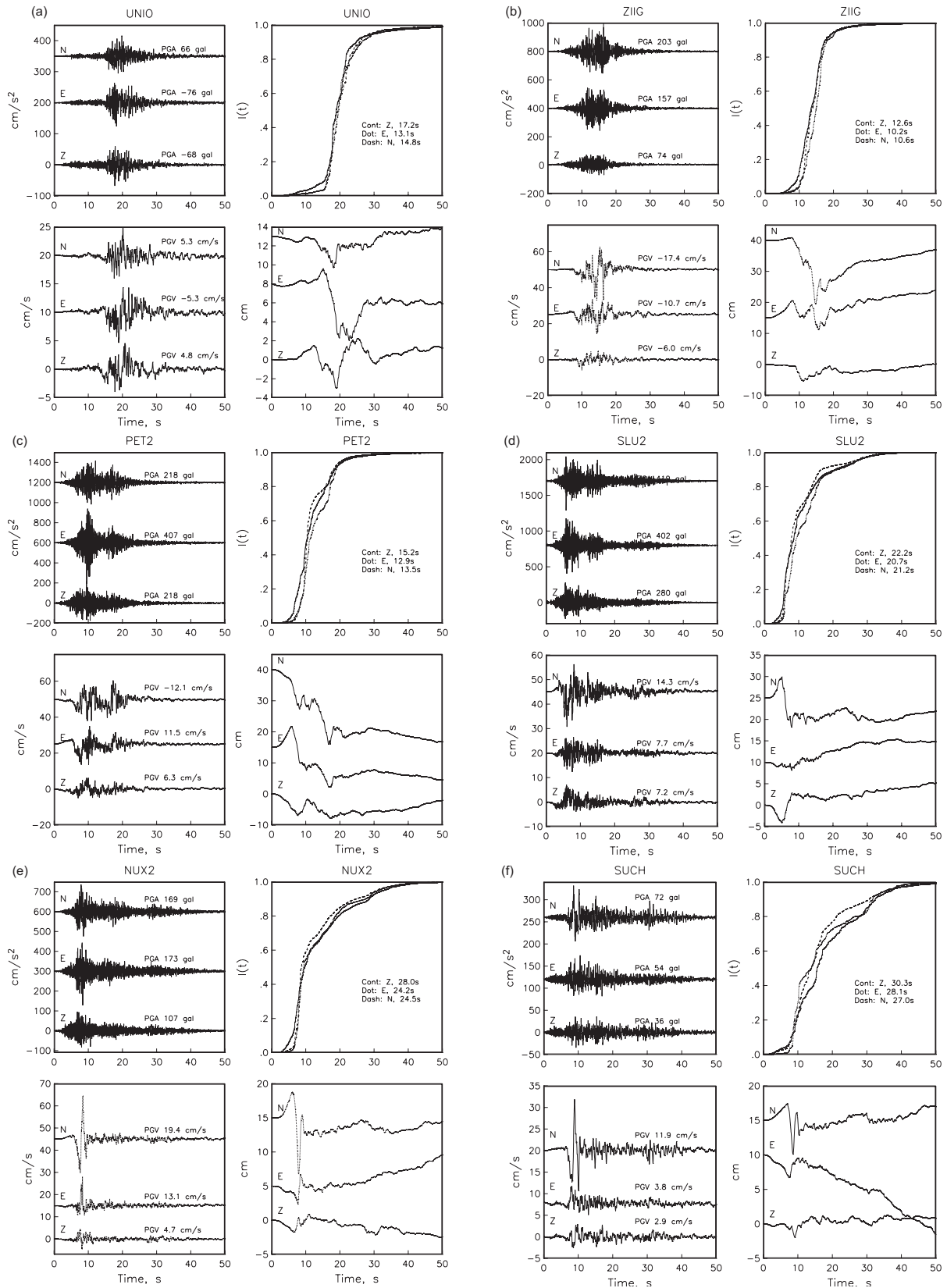
Figure 4. Acceleration, Arias intensity, velocity, and displacement at (a) UNIO, (b) ZIIG, (c) PET2, (d) SLU2, (e) NUX2, (f) SUCH, and (g) CAIG. Displacement was obtained from double integration of base-line corrected acceleration, without applying any filter.

29 Rayleigh waves and 29 Love waves. In addition, we included the static displacement measured by the GPS instruments of the SSN at ZIIG (Figure 5) and Tecpan (TCPN, which was taken as zero) in the inversion. We used the hypocenter location and origin time determined in this study (Table 1) as well as that reported initially by the SSN (Table 1). We inverted for the magnitude, direction and duration of slip at each 10×10 km^2 subpatch of the fault. The slip-rate function of each fault was parameterized by an asymmetric cosine function (Ji *et al.*, 2002a). The timing of the initial slip in each patch was constrained to follow a rupture velocity of 2-3 km/s. First the body-wave arrivals were aligned on theoretical travel times based on a 1D Earth model. However, we found large apparent time shifts between observed and calculated seismograms, caused by the 3D structure of the Earth. The systematic variation of these shifts with azimuth is probably also responsible for the large mislocation of the hypocenter by global agencies, mentioned above. To minimize the effect of unmodeled 3D structure on the result, we manually aligned the body-wave phases on the first observable arrival in the

seismogram. At stations where we could not identify the first arrival, we aligned them to be consistent with neighboring stations. The distribution of slip on the fault plane determined by the inversion, projected to the surface of the earth, is shown in Figure 6a and b. The figure also shows computed and observed static field at Zihuatanejo (ZIIG) and Tecpan (TECP). Observed and synthetic seismograms are compared in Figure 6c. The observations are well fit by the synthetics. The total seismic moment obtained from the modeling is 8.32×10^{19} Nm (M_w7.2).

There are two significant regions of slip, one near the hypocenter and the other ~ 40 km to WSW (Figure 6a). The first slip area is similar to that reported by NEIC and C. Mendoza but the second one is more concentrated than in the other two studies. The location of this area suggests that it probably corresponds to the third burst of high-frequency energy, seen in the accelerograms at SLU2, NUX2 and SUCH. The region of the second emission of high-frequency energy is not resolved in the inversion.

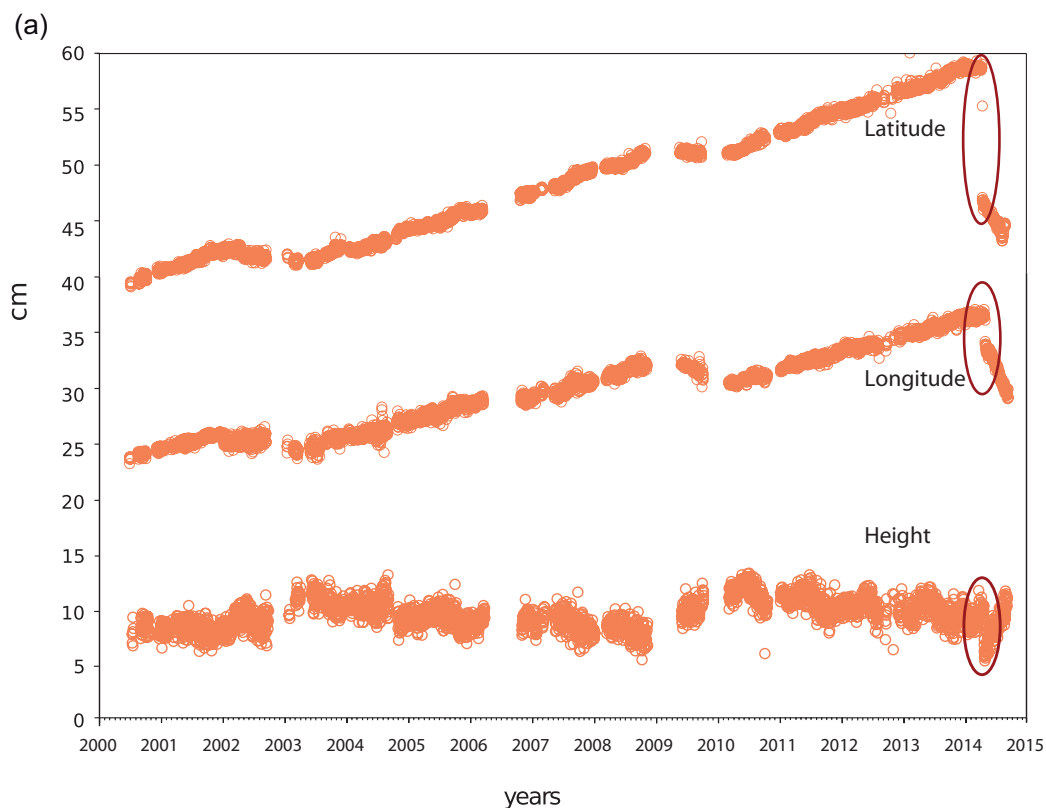
Figure 5. (a) GPS time series at ZIHU for the period 2000 – August 2014 (sampling 0.03 Hz). The ellipses enclose co-seismic displacement for the 18 April 2014 earthquake. Post-seismic displacement associated with the event is clearly visible.
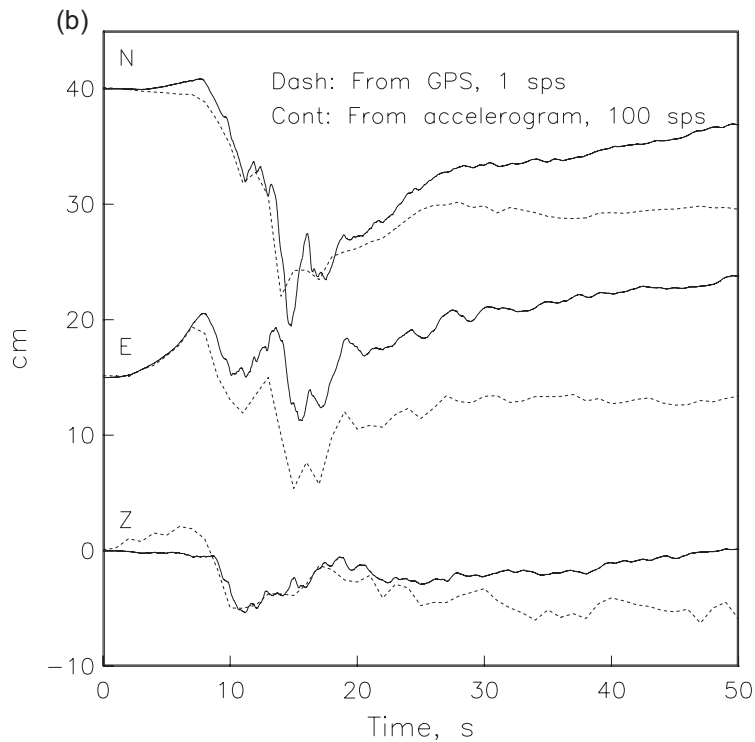
(b)

Figure 5. (b) Coseismic displacement at ZIIG from double integration of acceleration traces (sampling 100 Hz) and at ZIHU from 1-sec GPS data (ZIIG and ZIHU are collocated).

A comparison between the slip models obtained using the hypocenter determined in this study (Figure 6a) *versus* that reported initially by SSN (Figure 6b), shows that the relative location of the slip patches to the hypocenter and each other remains similar. However, the absolute location varies significantly. This shows how critical an accurate hypocenter location is.

Aftershocks of the 18 April 2014 earthquake

Following the earthquake, the Institutes of Geophysics and Engineering of UNAM installed a portable network of three broadband seismographs and two accelerographs in the epicentral zone. This network became operational within about 24 hours. Analysis of the data from this network is in progress. In this report we present location of the aftershocks based only on the permanent seismic network. We located 108 aftershocks ($2.4 \leq M \leq 5.2$), which occurred within 36 hours of the mainshock. In locating the earthquake we also used the azimuth of the source obtained from *P*-wave polarization. Keeping the depth free or fixing it at 15 km only slightly changed the epicentral locations. The aftershocks (from our preferred depth-free locations) define an area of ~ 40 km × 70 km, with major length oriented N75ºE, situated between Papanoa and Zihuatanejo

(Figure 6). This area encloses the inverted slip region. However, there were few aftershocks in the area of large slip corresponding to the first subevent. Aftershocks suggest that the rupture reached inland and extended ~ 30 km updip from the hypocenter. About 50 % of the aftershock area lies onshore. Generally, the aftershock and slip distributions are consistent with each other. A large fraction of the 2014 aftershock area overlaps with that of the 1979 earthquake (Figure 6a). A small part also falls in the aftershock area of the 21 September 1985 earthquake.

The slip contours during SSEs of 2001-2002, 2006, and 2009-2010 (adopted from Radiguet *et al.*, 2012) are shown in Figures 7a, 7b, and 7c along with the aftershock areas of large earthquakes in the region. The figure shows that the area of large slip during first subevent of the 2014 earthquake (located inland, Figure 6a) had previously slipped 6 - 10 cm, ~ 2 cm, and 6 – 10 cm during these previous SSE episodes.

The two largest aftershocks occurred on 8 May (M_w6.5) and 10 May (M_w6.1). During 8 May earthquake a bridge in Tecpan collapsed. The earthquake was strongly felt in Mexico City. The source parameters of these events are listed in Table 2. A careful analysis of spectral ratios of the recordings of these aftershocks shows
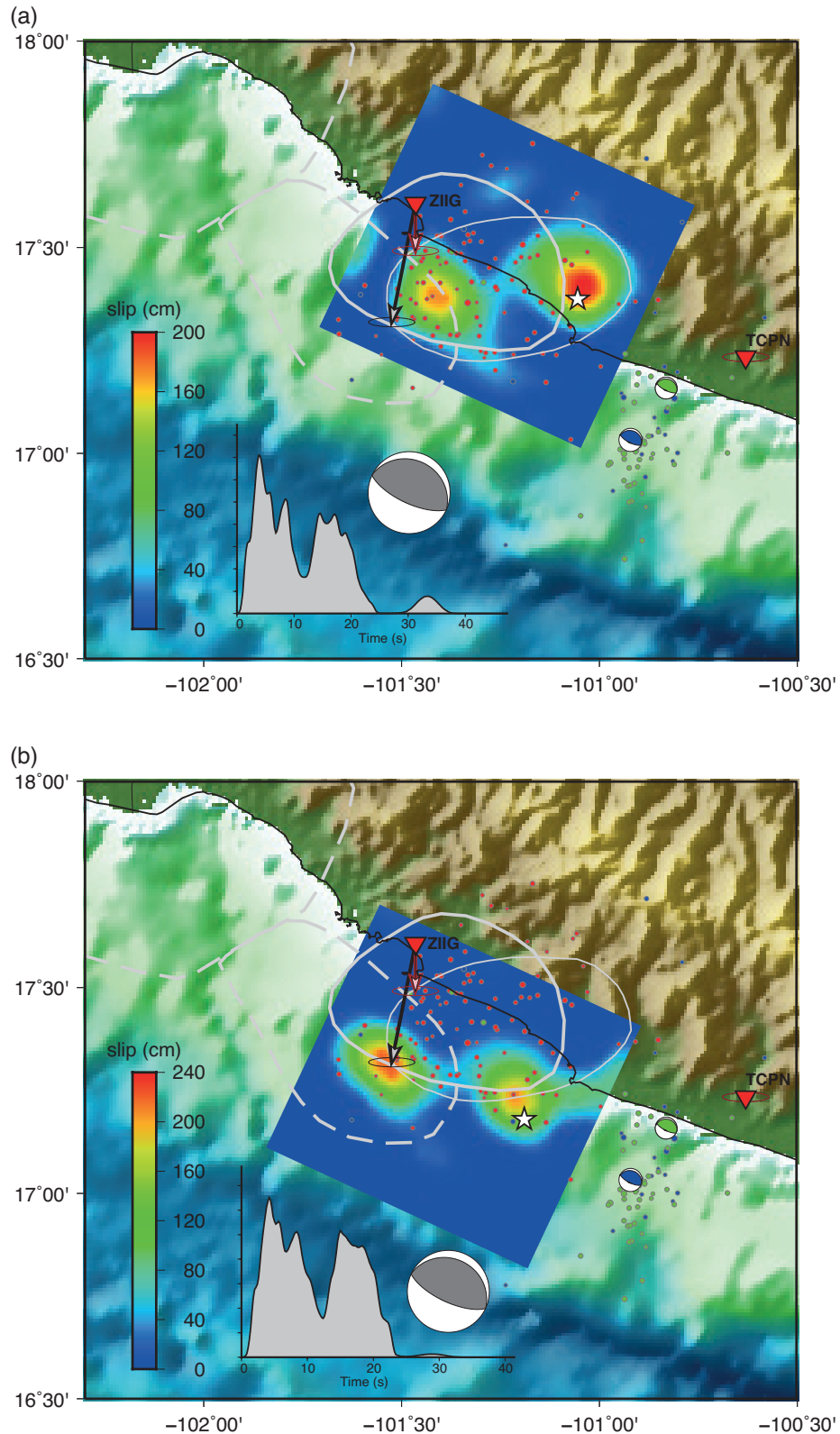
Figure 6. (a) Slip of the fault from inversion of teleseismic body and surface waves, and static field at ZIIG and Tecpan using hypocentral location from this study (Table 1). Circles: aftershocks (see text). Source time function for the solution is shown. (b) Same as (a) but using hypocentral location initially reported by SSN.

Figure 6. (c) Comparison of observed and synthetic teleseismic seismograms corresponding to the inversion using hypocentral location from this study.

that the rupture during the 8 May earthquake propagated SE, towards Acapulco, whereas the opposite occurred during the 10 May event. For the sake of brevity, we abstain from presenting a detailed analysis here. These aftershocks generated their own aftershock sequences. As seen in Figure 6, the location of these events and their aftershocks are separated from the aftershock and slip areas of the mainshock.

Clearly these two large aftershocks occurred in the NW Guerrero seismic gap.

SSE of 2014 and the Papanoa earthquake

As mentioned earlier, a slow slip event was in progress in Guerrero at the time of the Papanoa earthquake. Location of some selected GPS stations and the corresponding GPS time series

Table 2. Source parameters of the aftershocks of 8 May 2014 (Mw6.5) and 10 May 2014 (Mw6.1)

Date; Hr:Min:Sec	Lat., °N	Lon., °W	Depth, km	M_0, Nm	M_w	Strike, °	Dip, °	Rake, °	Source
08/05/14; 17:00:16.0	17.033	100.922	18F	$9.64 \times 10^{18+}$	6.6^+	297^+	11^+	89^+	This study
08/05/14; 17:00:22.1	17.300	100.690	23.2	6.67×10^{18}	6.5	289	21	83	Global CMT
10/05/14; 07:36:01.4	17.159	100.831	24.0	$2.19 \times 10^{18+}$	6.2^+	296^+	10^+	94^+	This study
10/05/14; 07:36:06.8	17.300	100.730	20.9	1.86×10^{18}	6.1	283	19	76	Global CMT

are shown in Figures 8a and 8b, respectively. Clearly, slip during the 2014 SSE extended to the north at least until IGUA (Iguala) and to the south upto the coastal stations of CAYA, COYU, ACYA, and TCPN. A visual examination of the traces in Figure 8b suggests that the SSE may have started near ACYA. As expected, large coseismic displacement caused by the 2014 Papanoa earthquake is observed at station ZIHP (see, also, Figure 5) and PAPA which lie above the rupture area. It is also visible at sites outside the epicentral zone, e.g., at TCPN, CAYA, and IGUA. Curiously, ZIHP shows small, if any, displacement during the SSE prior to the earthquake. This may also be true for PAPA, although the data was lost during the critical time period. It seems very likely that the region of seismic slip during the mainshock did not experience slow slip during the 2014 SSE prior to the rupture. Whether 2014 earthquake was triggered by the 2014 SSE must await mapping of the slip evolution in time and space which is currently in progress.

Radiated seismic energy and source spectrum

Seismic energy, E_s, for the mainshock was estimated from teleseismic (8.5×10^{14} J, $M_e = 7.03$) and regional data (3.1×10^{15} J, with corresponding energy magnitude $M_e = 7.43$) independently. For the first, we follow Boatwright and Choy's (1986) methodology as modified by Pérez-Campos and Beroza (2001) and Pérez-Campos *et al*. (2003).This includes a stronger attenuation correction for subduction earthquakes and a generic site correction for hard rock sites (Boore and Joyner, 1997). For the regional estimation, we followed Singh and Ordaz (1994), and included a site correction suggested by Pérez-Campos *et al*. (2003). Difference between these two estimates, a factor of 3.6, is reflected in the source spectra obtained from each set of data (Figure 9b). The teleseismic spectrum is depleted at high frequencies with respect to the regional spectrum. One possible explanation is that some energy is being trapped in the hanging wall (Brune, 1996), resulting in larger values of E_s for the regional estimates and lower values of E_s for stations in an azimuthal range of 0-150º than for stations within a range of 260-360º (Figure 9a). If we use regional stations within 260-360º of azimuth, we obtained an average $E_s = 1.08 \times 10^{15}$ J ($M_e = 7.12$), only a factor of 1.3 from the teleseismic estimate. Another possible explanation is directivity. Although understanding the cause of the discrepancy between teleseismic and regional estimates of E_s has important implication in ground motion prediction, it is beyond the scope of this paper.
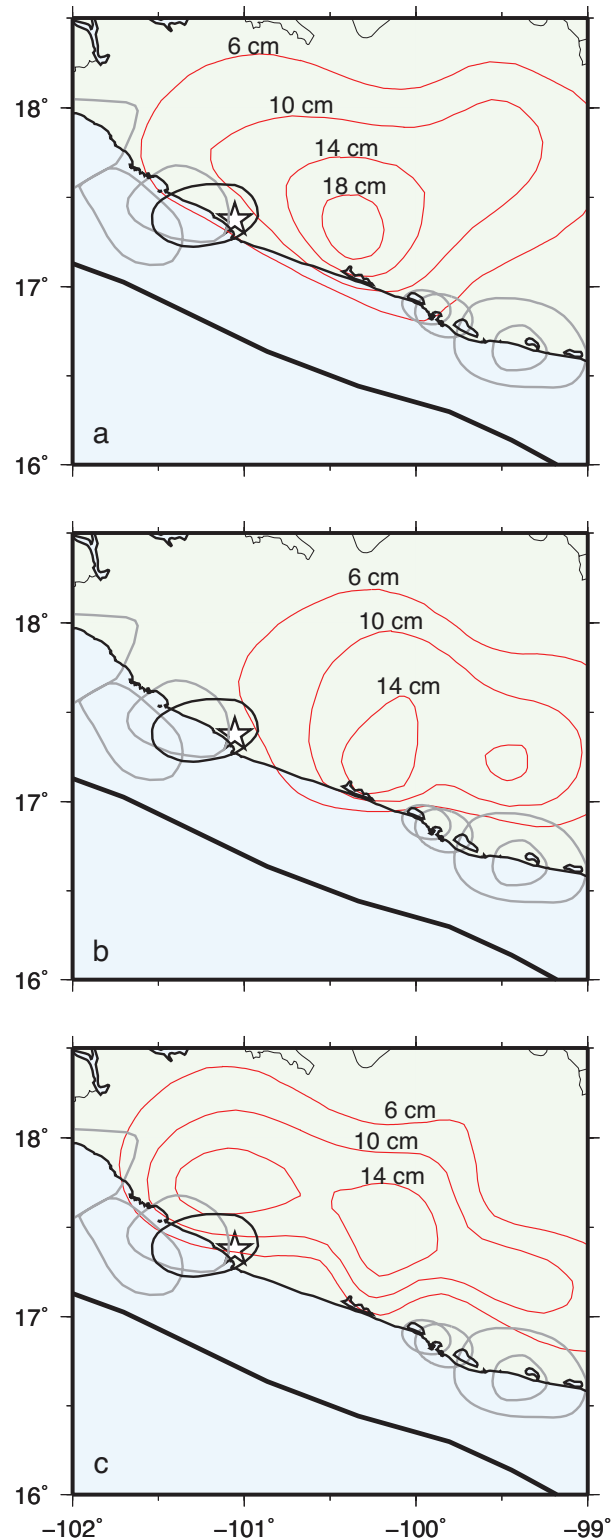

Figure 7. Slip contours (thin lines) during seismic slip events of (a) 2001-2002, (b) 2006, and (c) 2009-2010 adopted from Radiguet *et al*. (2012) for geometry B of the plate interface. The aftershock areas of large earthquakes in the region are shown by thick contours. Star denotes the epicenter of the 2014 earthquake.
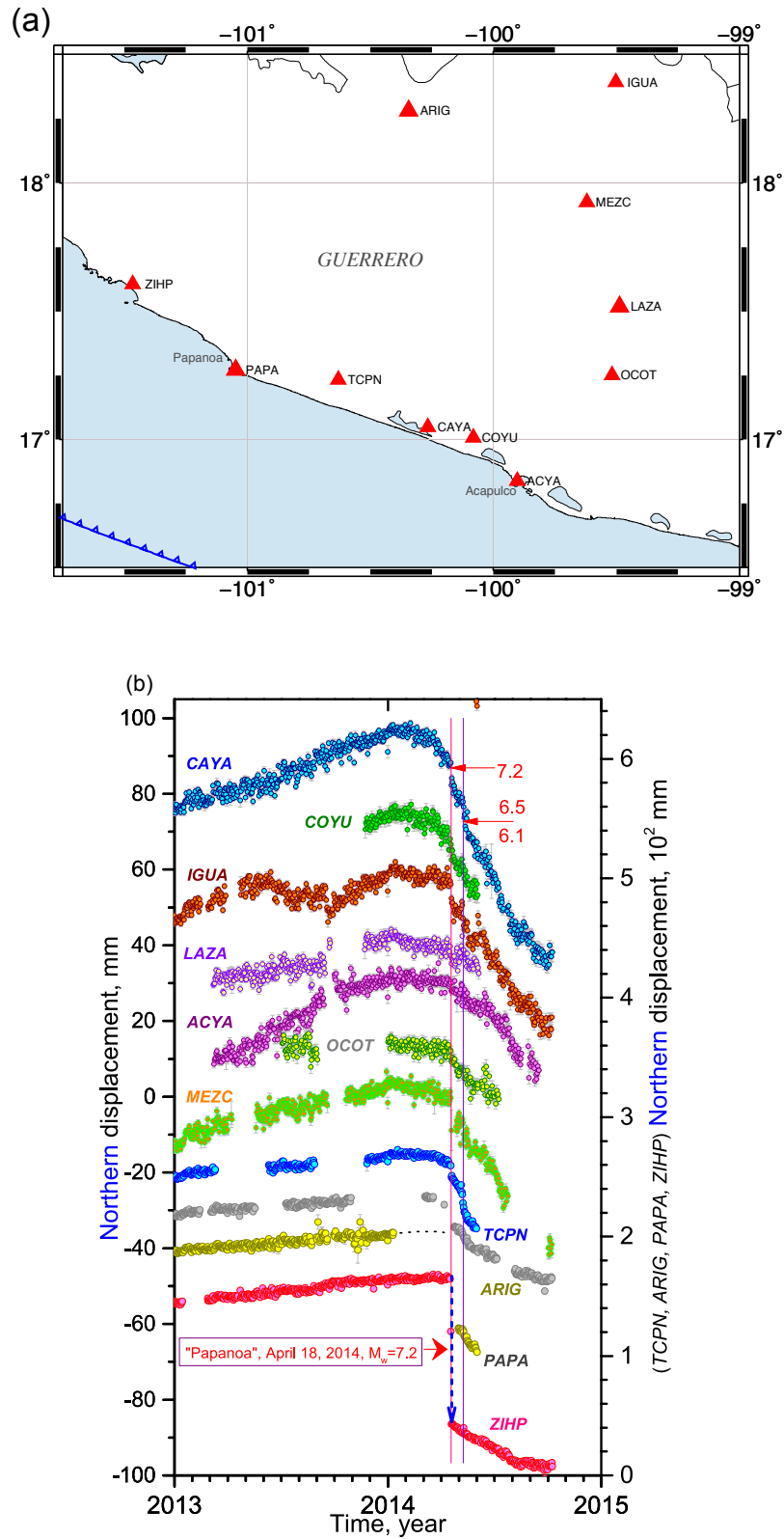
Figure 8. (a) Map showing location of some GPS sites in Guerrero. (b) Northern displacement beginning 2013 at sites shown in (a). Vertical lines indicate origin times of 18 April 2014 Papanoa earthquake and its largest aftershock of 8 May. Beginning of SSE in January of 2014 is visible at most stations, except at ZIHP and perhaps also at PAPA.
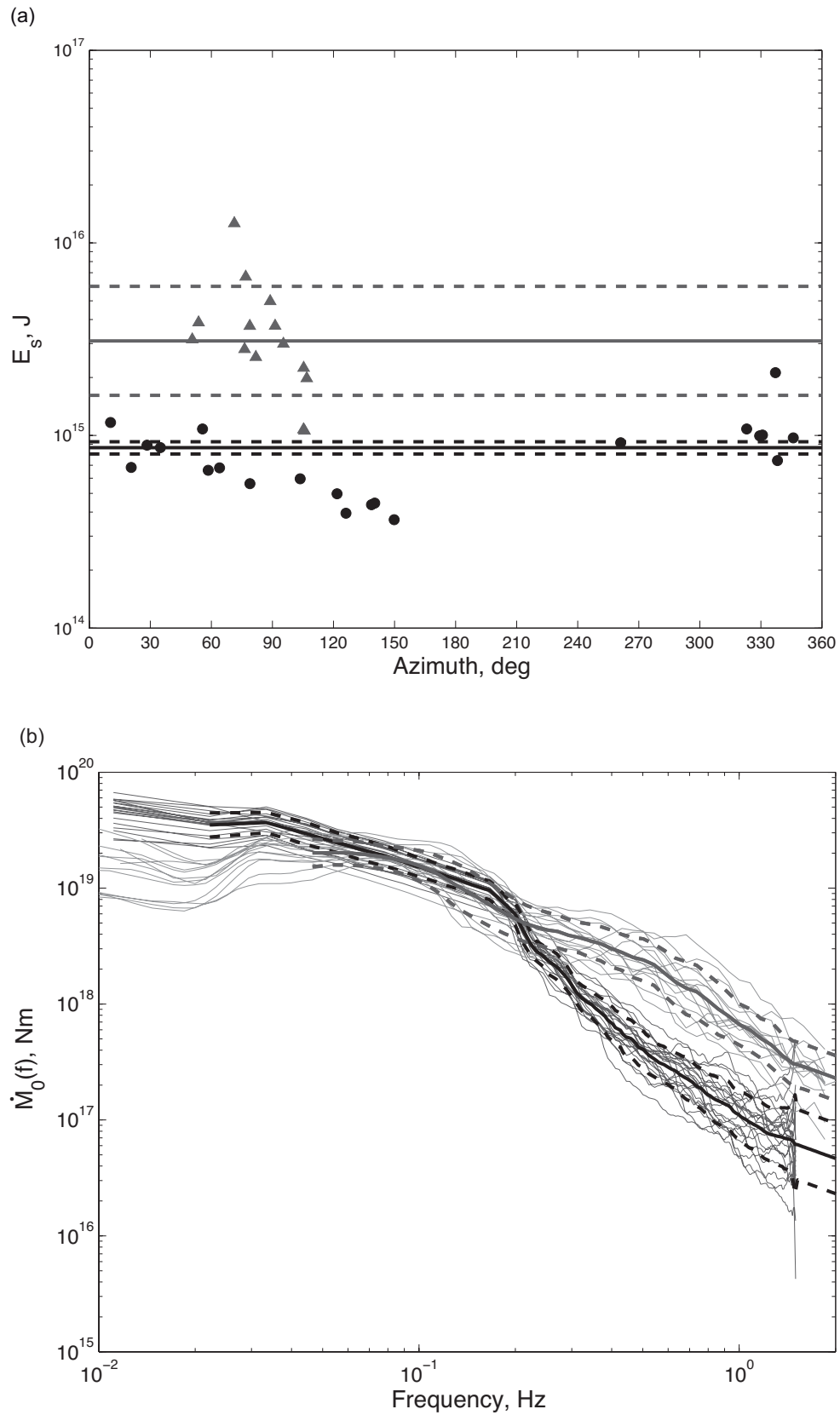
(a)

(b)

Figure 9. (a) Seismic energy, E_s, estimated with teleseismic data (black dots) and regional data (triangles). (b) Source spectra from teleseismic data (black lines) and regional data (gray lines).

Strong ground motions in Mexico City

The earthquake was strongly felt in Mexico City and caused general panic. The damage, however, was minor. Several walls collapsed and cracks were reported in some facades. The city suffered partial power outage. It is interesting to compare ground motions in Mexico City during this earthquake with those recorded during other recent large earthquakes. We illustrate this comparison at CU and SCT, representative sites of hill- and lake-bed zones, respectively.

Accelerograms of Mexican earthquakes recorded on CU campus of UNAM are available since 1964. *PGA* ($\mathrm{PGA} = \left[(A_n^2 + A_e^2)/2\right]^{1/2}$), where A_n and A_e are peak accelerations on NS and EW components, respectively) during the Papanoa earthquake was 13.7 gal, the fourth largest produced by interplate subduction earthquakes since 1964. The other three earthquakes were: 19 September 1985 Michoacán, M_w8.0 (30 gal); 14 March 1979 Petatlán, M_w7.4 (18.3 gal); and 21 September 1985 Michoacán-Guerrero, M_w7.5 (13.9 gal). Figure 10a shows the median Fourier spectra of the two horizontal components. The spectral amplitudes of all four events are about the same above 2 Hz. However, the 19 September 1985 earthquake has significantly higher spectral level below

2 Hz, followed by the 1979 earthquake. The spectra of the earthquakes of 21 Sep. 1985 and 2014 are similar above 0.4 Hz and the *PGA* values are almost same.

SCT station, located in the lake-bed zone, did not exist in 1979 and the accelerograph malfunctioned during the 21 Sep. 1985 earthquake. Figure 10b shows median Fourier spectra of four interplate earthquakes with largest recorded *PGA* at SCT. These events are: 19 Sep. 1985 Michoacán, M_w8.0 (132.1 gal); 25 Apr. 1989 San Marcos, M_w6.9 (38.8 gal); 18 Apr. 2014, M_w7.3 (31.3 gal); and 14 Sep. 1995, Copala, M_w7.3 (29.5 gal). The spectral level of the 19 Sep. 1985 is higher than for the other events. 1989 earthquake has slightly higher spectral level between 0.2 and 0.6 Hz than the other two events, which have very similar spectra as well as *PGA* values.

We recall that during the 1979 earthquake a building of Iberoamericana University in the lake-bed zone collapsed. *PGA* during this earthquake at CU was 18 gal. The earthquake of 1989 caused some damage to the city. During the 1989 earthquake the *PGA* values were 12 and 39 gals at CU and SCT, respectively. This suggests that some damage to Mexico City from an interplate earthquake may be expected if *PGA* values at CU and/or SCT exceed ~ 15 and
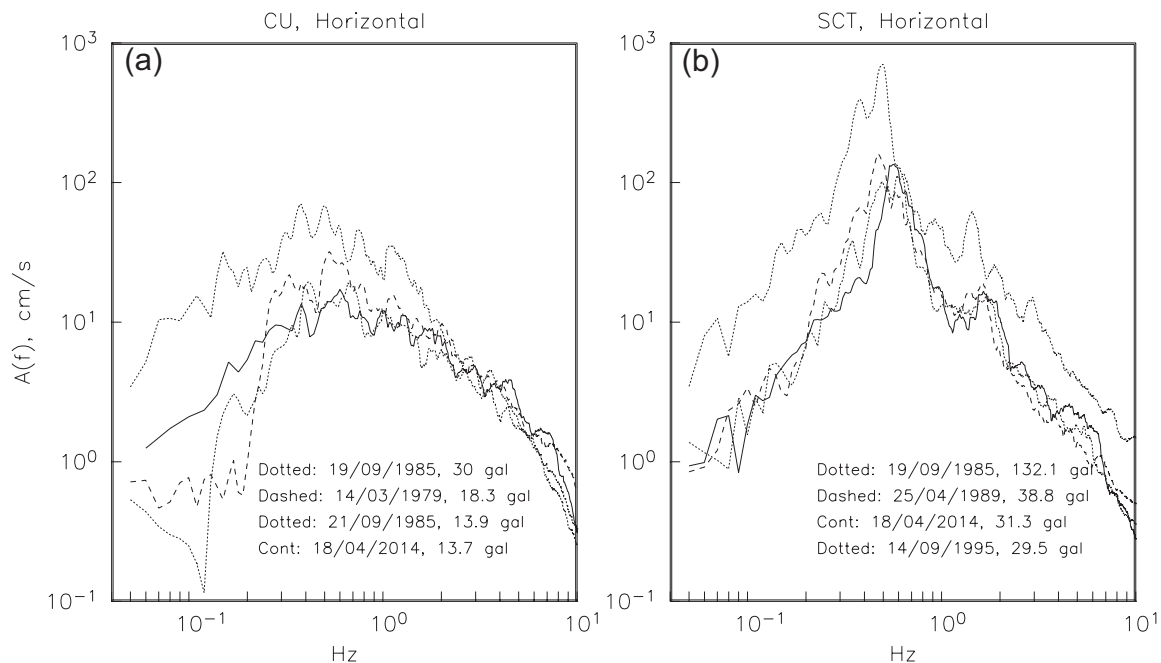

Figure 10. (a) Fourier acceleration spectra (median of the two horizontal components) at CU, a hill-zone site, during four interplate earthquakes with largest PGA values recorded at the station since 1964. PGA values are given in the figure. (b) Same as (a) but at SCT, a lake-bed zone site.

40 gal, respectively. It is worth remembering that these values at CU and SCT during the disastrous 19 September 1985 earthquakes were 30 and 132 gals, respectively.

Damage and Iso-Acceleration Contours

The earthquake caused significant damage to Papanoa and other coastal towns in the epicentral zone. The highest *PGA* (geometric mean of the two horizontal components) of 1138 gal was recorded at a soft site in Papanoa. At hard sites the recorded *PGA*s were ≤ 420 gal (Figure 4). Figure 11 shows PGA contours of the earthquake. These contours were obtained from the recorded data using a Bayesian interpolation technique. We note that the maximum contour roughly coincides with the maximum slip (Figure 6a). The figure also shows municipalities where significant structural damage occurred and which received federal funds for recovery and reconstruction of the affected population.

Attenuation of strong motion with distance

Figure 12 shows plot of ground motion parameters - *PGA* and pseudo-acceleration response spectra (5 % damping), *Sa*, at *f* = 5, 1, and 0.5 Hz - as a function of *R*, the closest distance from the rupture area. With few

exceptions (marked in the figure), the stations are situated at hardrock sites. The expected motions from ground-motion prediction equations (GMPEs) developed by Arroyo *et al*. (2010), shown by dashed curves (median and ± 2σ), match well with the observations, giving us confidence in the applicability of these relations.

Discussion and conclusions

The earthquake of 2014 ruptured a segment of the plate boundary between Papanoa and Zihuatanejo, leaving intact the NW Guerrero seismic gap, which extends from Acapulco to Papanoa (~100 ºW– 101 ºW). More than half of the aftershock area of the earthquake overlaps with that of the 1979 earthquake and a small fraction of it with that of the 21 September 1985 earthquake. The aftershock area of the 1985 earthquake is somewhat uncertain as it generated relatively few aftershocks and also because of the contamination from the aftershocks of the great Michoacán earthquake (M_w8.0) which had occurred ~36 hours earlier (UNAM Seismology Group, 1986). Due to a dense deployment of portable seismographs in the epicentral zone, the 1979 aftershock area is well defined (e.g., Valdés-González *et al*., 1998). Unfortunately, the slip distribution during these previous earthquakes is not
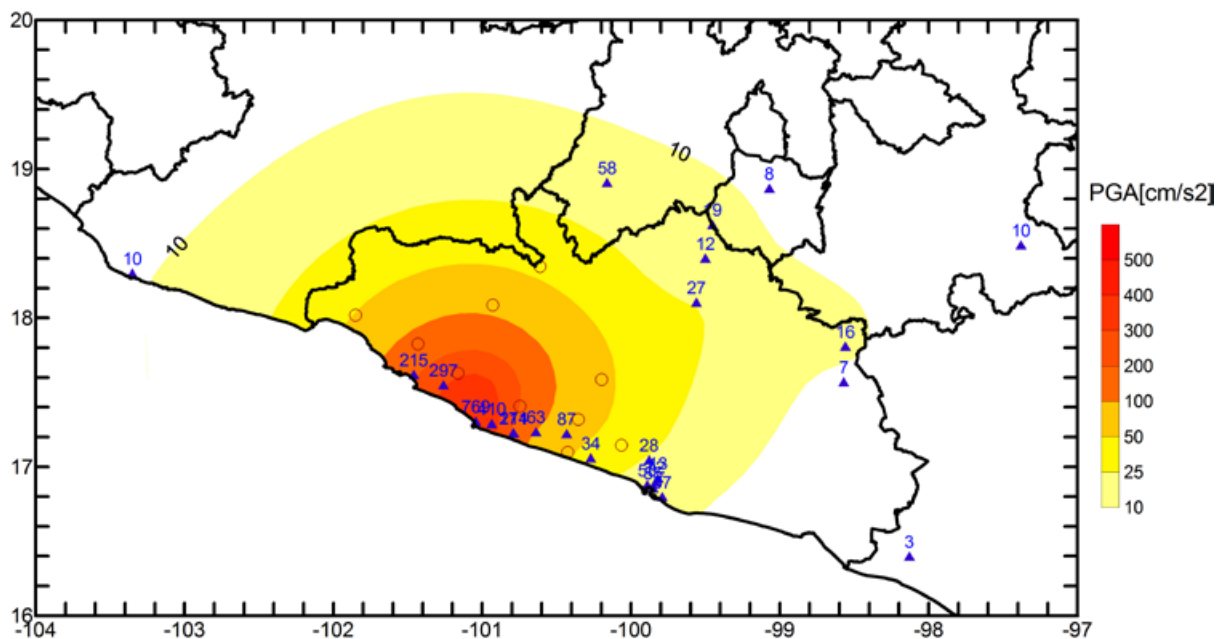

Figure 11. PGA iso-contour for rock sites during the Papanoa earthquake. Triangles: recording stations. Circles: municipalities where considerable structural damage was observed.

known. For this reason, a critical issue that cannot be resolved is whether one or both patches that slipped during the 2014 event also broke during 1979 and/or 1985, or whether the major slip during 2014 occurred over areas that had not slipped during the previous two earthquakes. In view of the aftershock areas of the three earthquakes, the width of the seismogenic zone in the region may be ~ 70 km, extending ~ 25 km inland.

The adjacent segment, the NW Guerrero gap, has not experienced a large/great earthquake since 1911. Episodic slow slip earthquakes (SSEs) reported in the region occur not only on the subhorizontal part of the plate interface but appear to extend updip up to about 10 km inland from the coast. Large slip during the first subevent of the Papanoa earthquake occurred on a patch of the plate interface which had slipped 6 – 10 cm, ~ 2 cm, and 6 – 10 cm during previous SSE episodes of 2001-2002,
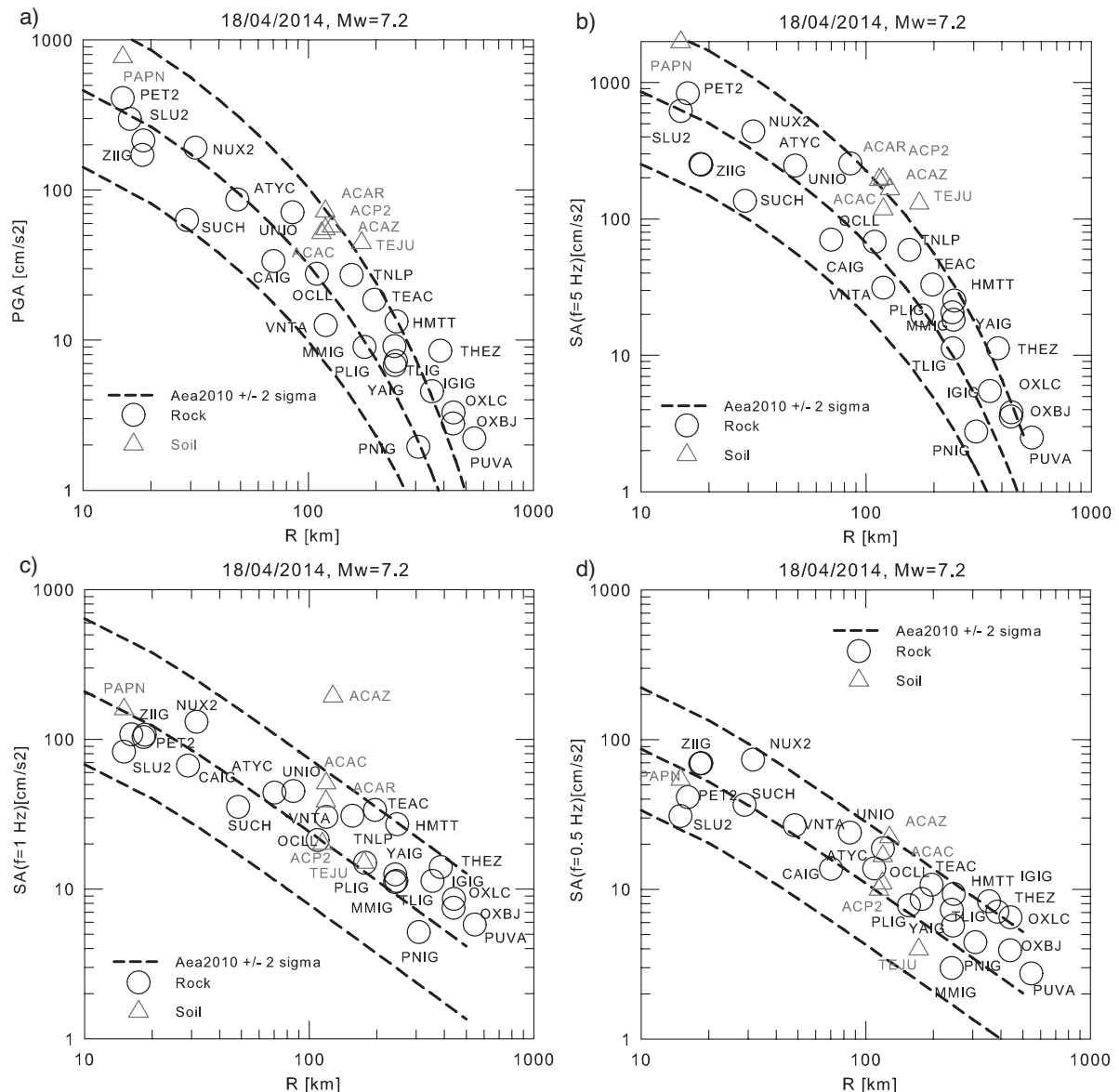

Figure 12. PGA and pseudo-acceleration response spectra (5% damping), Sa, at f = 5, 1, and 0.5 Hz, as a function of R (closest distance to rupture area), observed during the Papanoa earthquake. PGA and Sa values correspond to the geometrical mean of the two horizontal components. Predictions from Arroyo *et al.* (2010) (denoted as Aea2010) shown by dashed curves (median and ± 2σ) match well with the observations. Note that only the intra-event part of sigma is considered.

2006, and 2009-2010, respectively (Radiguet *et al.*, 2012) (Figure 7). The inverted slips on/near the patch during the SSEs are mostly controlled by the GPS station at Zihuatanejo (ZIHU) and are probably not well resolved. If, however, the slip on the patch during the SSEs is real, then it implies that slow and fast slip can occur over the same area of the interface during SSEs and earthquakes, respectively.

Mechanical models of earthquakes under rate- and state-dependent (R&S) laws show that rapid (unstable) and aseismic slip is primarily governed by velocity-weakening (VW) and velocity-strengthening (VS) fault constitutive regimes, respectively (e.g., Lapusta *et al.*, 2000; Liu and Rice, 2007; Kaneko *et al.*, 2010). Since the aseismic slip apparently spread over the first asperity of the Papanoa earthquake during earlier SSE episodes, it suggests that this segment is mainly characterized by VS properties. However, while unstable rupture propagation (with rapid slip) may occur over VS segments due to dynamically driven weakening processes (Noda and Lapusta, 2013), it cannot spontaneously initiate in those segments. To reconcile the observations with a physical model, we propose that the area which ruptured during the first subevent was a VW patch (an asperity) surrounded by a conditionally stable and larger VS zone where slow slip during the SSEs occurs. This R&S mechanism has successfully explained the mechanism of repeating earthquakes (Chen and Lapusta, 2009), where slow slip in VW patches arises as a consequence of aseismic movement in the surrounding VS fault.

We note that the aftershock areas (presumably also the slip areas) of 1979 and 2014 earthquakes begin about ~ 35 km downdip from the trench (Figure 6a). Seismically, the interface from the trench up to a distance of ~35 km downdip appears similar to that of the adjacent NW Guerrero gap (Figure 1b). In both regions there is little seismicity at $M >$ 5 level in this portion of the interface, except for a sequence of near-trench earthquakes which were recorded on 18 April 2002. The mainshock (M_w6.7), which was located near the trench of the NW Guerrero gap, produced many aftershocks. The principal aftershock (M_w5.9) was also located near the trench but updip of the 1979 and 2014 aftershock areas. The two events are denoted NTE in Figure 1b. These moderate earthquakes were deficient in high-frequency radiation of seismic energy (Iglesias *et al.*, 2003). The mainshock had extraordinarily large centroid delay time for its magnitude, about 30 s (Figure 4 of Duputel *et al.*, 2013). It also generated a small tsunami.

These characteristics point to a tsunami earthquake. [The only other region along the Mexican subduction zone where similar near-trench earthquakes have been documented is off the coast of Pinotepa Nacional (Iglesias *et al.*, 2003).] Thus, the shallow interface near the trench updip of the aftershock areas of 1979 and 2014 earthquakes as well as the NW Guerrero seismic gap seems to be in the domain of tsunami earthquakes or of stable sliding. The interface further downdip upto ~ 35 km from the trench may be aseismically stable, or conditionally stable so that it slips seismically when accelerated and dynamically weakened by rupture of adjacent seismic patches (Noda and Lapusta, 2013).The interface from 35 to 80 km of the trench in Papanoa – Zihuatanejo region clearly differs from the region of NW Guerrero. In the former region, although aseismic (slow) slip seems to reach the coast (~65 km from the trench), this seismically active portion of the interface clearly has highly locked VW asperities, so that the inter-SSE coupling ratio is relatively high (>0.5). In the latter region (i.e., within the seismic gap), the strain is mostly released during SSEs, the inter-SSE coupling ratio is very small (< 0.2), and slip deficit is one-fourth of that in the former region (Radiguet *et al.*, 2012). However, as suggested by the two largest aftershocks (M_w6.5 and M_w6.1) that occurred in the NW segment of the gap about 20 km away from the mainshock (Figure 6a), this portion of the interface may be conditionally stable with isolated unstable asperities, such as the ones depicted by the green and blue epicenters. Actually, the absence of aftershocks between this area and the main rupture zone may probably reflect aseismic afterslip accommodation on the plate interface that eventually triggered the M_w6.5 and M_w6.1 sequence.

The earthquake caused significant damage to Papanoa and other coastal towns. The peak iso-acceleration contour coincides with area of large-slip. The earthquake was strongly felt in Mexico City but caused only minor damage. The recorded ground motions in the city were similar to those produced by the 1979 and 1985 earthquakes. It is reassuring to note that the ground motion prediction equations developed for Mexico explain the observed ground motion parameters quite well.

Acknowledgements

earthquake in Mexico, the Group informally coordinates its efforts in data collection from autonomous stations, field deployment of seismographs and accelerographs, analysis of the data, and elaboration of a preliminary report. The credit of the work is shared by all.

References

Abe K., 1981, Magnitude of large shallow earthquakes from 1904 to 1980. *Phys. Earth. Planet. Interiors,* 27, 72- 92.

Abe K., Noguchi S.I., 1983, Revision of magnitudes of large shallow earthquakes, 1897–1912. *Phys. Earth. Planet. Interiors* 33, 1, 1-11.

Anderson J.G., Bodin P., Brune J.N., Prince J., Singh S.K., Quaas R., Onate M., 1986, Strong Ground Motion from the Michoacan, Mexico, Earthquake. *Science* 233, 4768, 1043-1049. DOI:10.1126/science.233.4768.1043.

Anderson J.G., Singh S.K., Espindola J.M., Yamamoto J., 1989, Seismic strain release in the Mexican subduction thrust. *Phys. Earth. Planet. Interiors* 58, 4, 307-322.

Anderson J.G., Brune J.N., Prince J., Quaas R., Singh S.K., Almora D., Bodin P., Oñate M., Vásquez R., Velasco J.M., 1994, The Guerrero accelerograph network. *Geofísica Internacional* 33, 341-372.

Arroyo D., Garcia D., Ordaz M., Mora M.A., Singh S.K., 2010, Strong ground-motion relations for Mexican intreplate earthquakes. *J. Seismol.*, DOI 10.1007/s10950-010-9200-0.

Boatwright J., Choy G.L., 1986, Teleseismic estimates of the energy radiated by shallow earthquakes. *J. Geophys.Res.* 91, B2, 2095-2112.

Boore D.M., Joyner W.B., 1997, Site amplifications for generic rock sites. *Bull. Seismol. Soc. Am.* 87, 2, 327-341.

Böse E., Villafaña A., García y García J., 1908, El temblor del 14 de abril de 1907. *Parergones del Instituto Geológico de México* II, 4, 5, 6, 135-258.

Brune J.N., 1996, Particle motions in a physical model of shallow angle thrust faulting. *Proceedings of the Indian Academy of Sciences-Earth and Planetary Sciences* 105, 2, 197-206.

Cavalié O., Pathier E., Radiguet M., Vergnolle M., Cotte N., Walpersdorf A., Kostoglodov V., Cotton F., 2013, Slow slip event in the Mexican subduction zone: Evidence of shallower slip in the Guerrero seismic gap for the 2006 event revealed by the joint inversion of InSAR and GPS data. *Earth Planet. Sc. Lett.* 367, 52–60.

Chen T., Lapusta N., 2009, Scaling of small repeating earthquakes explained by interaction of seismic and aseismic slip in a rate and state fault model. *J. Geophys. Res.,* 114, B01311.

Duputel Z., Tsai V.C., Rivera L., Kanamori H., 2013, Using centroid time-delays to characterize source durations and identify earthquakes with unique characteristics. *Earth Planet. Sc. Lett.* 374, 92-100, DOI 10.1016/j.epsl.2013.05.024.

Figueroa J., 1970, Catalogo de sismos ocurridos en la República Mexicana. Report No. 272, Instituto de Ingeniería, U.N.A.M., México.

García Acosta V., Suárez Reynoso G., 1996, *Los sismos en la historia de México*, tomo I. UNAM-CIESAS-Fondo de Cultura Económica, México, 718.

Gutenberg B., 1956, Great earthquakes 1896-1903.*Transactions, American Geophysical Union,* 37, 608-614.

Gutenberg B., Richter C.F., 1954, *Seismicity of the Earth and Associated Phenomena*, 2nd edition, Princeton University Press, Princeton, New Jersey, 310 pp.

Husker A., Davis P.M., 2009, Tomography and thermal state of the Cocos plate subduction beneath Mexico City. *J. Geophys. Res.,* 114, B04306 doi: 10.1029/2008JB006039.

Iglesias A., Singh S.K., Pacheco J.F., Alcántara L., Ortiz M., Ordaz M., 2003, Near-trench Mexican earthquakes have anomalously low peak accelerations. *Bull. Seism. Soc. Am.* 93, 2, 953–959,

Iglesias A., Singh S.K., Lowry A.R., Santoyo M., Kostoglodov V., Larson K.M., Franco-Sánchez S.I., 2004,The silent earthquake of 2002 in the Guerrero seismic gap, Mexico (Mw=7.6): Inversion of slip on the plate interface and some implications. *Geofísica Internacional,* 43, 3, 309-317.

Ji C., Wald D.J., Helmberger D.V., 2002a, Source description of the 1999 Hector Mine, California, earthquake, Part I: Wavelet domain inversion theory and resolution analysis. *Bull. Seismol. Soc. Am.,* 92, 1192-1207.

Ji C., Wald D.J., Helmberger D.V., 2002b, Source description of the 1999 Hector Mine, California, earthquake, Part II: Complexity of slip history. *Bull. Seismol. Soc. Am.* 92, 1208-1226.

Kaneko Y., Avouac J.P., Lapusta N., 2010, Towards inferring earthquake patterns from geodetic observations of interseismic coupling. *Nature Geoscience,* 3, 363-369.

Kim Y., Clayton R.W., Jackson J.M., 2010, Geometry and seismic properties of the subducting Cocos plate in central Mexico. *J. Geophys. Res.,* 115, B06310, doi:10.1029/2009JB006942.

Kostoglodov V., Singh S.K., Santiago J.A., Larson K.M., Lowry A.R., Bilham R., 2003, A large silent earthquake in the Guerrero seismic gap, Mexico. *Geophys. Res. Lett.,* 15, doi:10.1029/2003GL017219.

Kostoglodov V., Husker A., Shapiro N.M., Payero J.S., Campillo M., Cotte N., Clayton R., 2010, The 2006 slow slip event and nonvolcanic tremor in the Mexican subduction zone. *Geophys. Res. Lett.* 37, doi: 10.1029/2010GL045424.

Lapusta N., Rice J., Ben-Zion Y., Zheng G., 2000, Elastodynamic analysis for slow tectonic loading with spontaneous rupture episodes on faults with rate- and state-dependent friction. *J. Geophys. Res.,* 105, 23765–23789.

Liu Y., Rice J.R., 2007, Spontaneous and triggered aseismic deformation transients in a subduction fault model. *J. Geophys. Res.* 112, B09404, doi:10.1029/2007JB004930.

Lowry A.R., Larson K.M., Kostoglodov V., Bilham R., 2001, Transient fault slip in Guerrero, southern Mexico. *Geophys. Res. Lett.* 28, 3753– 3756.

Muñoz Lumbier M., 1935, Geografía sísmica (con aplicaciones a la República Mexicana). Contribución a la carta mundial de calamidades. Talleres Gráficos de la Nación, Secretaría de la economía Nacional, México.

Noda H., Lapusta N., 2013, Stable creeping fault segments can become destructive as a result of dynamic weakening. *Nature* 493, 518–521, doi:10.1038/nature11703.

Okada Y., 1992, Internal deformation due to shear and tensile faults in a half-space. *Bull. Seismol. Soc. Am.* 82, 2, 1018-1040.

Ortiz M., Singh S.K., Kostoglodov V., Pacheco J., 2000, Source areas of the Acapulco-San Marcos, Mexico earthquakes of 1962 (M 7.1; 7.0) and 1957 (M 7.7), as constrained by tsunami and uplift records. *Geofísica Internacional,* 39, 4, 337-348.

Pacheco J.F., Singh S.K., 2010, Seismicity and state of stress in Guerrero segment of the Mexican subduction zone. *J. Geophys. Res.* 115, B01303, doi: 10.1029/2009JB006453.

Pardo M., Suárez G., 1995, Shape of the subducted Rivera and Cocos plates in southern Mexico: seismic and tectonic implications. *J. Geophys. Res.,* 100, B7, 12,357-12,373.

Pérez-Campos, X., and G. C.Beroza (2001), An apparent mechanism dependence of radiated seismic energy. *J. Geophys. Res.* 106, No. B6, 11,127-11,136.

Pérez-Campos X., Singh S.K., Beroza G.C., 2003, Reconciling teleseismic and regional estimates of seismic energy. *Bull. Seismol. Soc. Am.,* 93, 5, 2123-2130.

Pérez-Campos X., Kim Y.H., Husker A., Davis P.M., Clayton R.W., Iglesias A., Pacheco J.F., Singh S.K., Manea V.C., Gurnis M., 2008, Horizontal subduction and truncation of the Cocos Plate beneath central Mexico. *Geophys. Res. Lett.* 35, 18, L18303.

Radiguet M., Cotton F., Vergnolle M., Campillo M., Valette B., Kostoglodov V., Cotte N., 2011, Spatial and temporal evolution of a long term slow slip event: The 2006 Guerrero Slow Slip Event. *Geophys. J. Int.* 184, 2, 816-828.

Radiguet M., Cotton F., Vergnolle M., Campillo M., Walpersdorf A., Cotte N., Kostoglodov V., 2012, Slow slip events and strain

accumulation in the Guerrero gap, Mexico. *J. Geophys. Res.* 117, 4, B04305.

Singh S.K., Dominguez T., Caştro R., Rodriguez M., 1984, P waveform of large, shallow earthquakes along the Mexican subduction zone. *Bull. Seismol.Soc. Am.,* 74, 6, 2135-2156.

Singh S.K., Astiz L., Havskov J., 1981, Seismic gaps and recurrence periods of largeearthquakes along the Mexican subduction zone: A reexamination. *Bull. Seismol. Soc. Am.,* 71, 827-843.

Singh S.K., Ordaz M., 1994, Seismic energy release in Mexican subduction zone earthquakes. *Bull. Seismol. Soc. Am.* 84, 5, 1533-1550.

Singh S.K., Pardo M., 1993, Geometry of the Benioff zone and state of stress in the overriding plate in central Mexico. *Geophys. Res. Lett.* 20, 14, 1483-1486.

Singh S.K., Pérez-Campos X., Iglesias A., Melgar D., 2012, A method for rapid estimation of moment magnitude for early tsunami warning based on coastal GPS networks. *Seismol. Res. Lett.,* 83, 3, 516-530.

Singh S.K., Suárez G., Domínguez T., 1985, The Oaxaca, Mexico, earthquake of 1931: lithospheric normal faulting in the subducted Cocos plate. *Nature,* 317, 6032, 56-58.

Song T.-R.A., Helmberger D.V., Brudzinski M.R., Clayton R.W., Davis P., Pérez-Campos X., Singh S.K., 2009, Subducting slab ultra-slow velocity layer coincident with silent earthquakes in southern Mexico. *Science* 324, 5926, 502-506.

Suárez G., Monfret T., Wittlinger G., David C. 1990, Geometry of subduction and depth of the seismogenic zone in the Guerrero gap, Mexico. *Nature,* 345, 6273, 336-338.

UNAM Seismology Group, 1986, The September 1985 Michoacan earthquakes: Aftershock distribution and history of rupture. *Geophys. Res. Lett.,* 13, 573-576.

Valdés-González C., Novelo-Casanova D.A., 1998, The western Guerrero, Mexico, seismogenic zone from the microseismicity associated to the 1979 Petatlan and 1985 Zihuatanejo earthquakes. *Tectonophysics,* 287, 271-277.

Yoshioka S., Mikumo T., Kostoglodov V., Larson K.M., Lowry A.R., Singh S.K., 2004, Interplate coupling and a recent aseismic slow slip event in the Guerrero seismic gap of the Mexican subduction zone, as deduced from GPS data inversion using a Bayesian information criterion. *Phys. Earth. Planet. Interiors,* 146, 3, 513-530.

Appendix A

Notes on large earthquakes in Guerrero, 1989-1911

Seven large earthquakes occurred along the Guerrero segment of the Mexican subduction zone between 1899 and 1911. Location and magnitude of these events reported in different catalogs differ significantly. Here we very briefly summarize some relevant information regarding each of these events and give our preferred location and magnitude in Table A1. Unless otherwise mentioned, our preferred surface-wave magnitude, M_S, is the one listed in the catalog of large shallow earthquakes of Abe and Noguchi (1983) who reevaluated M_S of earthquakes for the period 1899-1912. This catalog is based on calibration of undamped Milne seismographs and original worksheets of Gutenberg and Richter (see Abe and Noguchi, 1983 for details). Anderson *et al*. (1989) estimated seismic moment of large earthquakes in the period 1907-1957 from Wiechert seismograms recorded at Uppsala. Table A1 also lists moment magnitude, M_w, if available. The felt and damage reports, with emphasis on the coastal areas, are very briefly mentioned below. These are extracted from García Acosta and Suárez Reynoso (1996) who provide an exhaustive description of earthquakes in Mexico. Our preferred locations are subjective, relying mostly upon the description of damage and felt reports.

14 January 1899, 23:43. The earthquake was strongly felt in the entire state of Guerrero. It was very strongly felt in Tecpan, destroying 33 houses, prefecture, city hall, and schools. It was also felt very strongly in Zihuatanejo where the sea inundated the coast by 35 m. Based on limited intensity data, Singh *et al*. (1981) had previously assigned the event an epicenter of 17.1 ºN, 100.5 ºW and a magnitude of 7.9. Gutenberg (1956) reported the location as 17 ºN, 98 ºW (with estimated limit of error of ± 5º) and a unified magnitude m of 7.8. M_S listed in the catalog of Abe and Noguchi (1983) is 7.5, which, as mentioned earlier, is our preferred magnitude. Since the epicenter of 17.1 ºN, 100.5 ºW (Singh *et al*., 1981) is consistent with the extensivedamage reports compiled by García Acosta and Suárez Reynoso (1996); we think that this location is reasonably accurate.

15 April 1907, 06:08. An excellent, detailed study on this earthquake was published by Böse *et al*. (1908).The earthquake was felt over an extensive area of the republic. It caused severe damage in many towns of Guerrero,

especially in Acapulco, San Marcos, Chilapa, and Chilpancingo. The sea inundated the coast in Acapulco. The epicenter listed in Gutenberg and Richter (1954) is 17 ºN, 100 ºW. The epicentral zone outlined by Böse *et al*. (1908) is consistent with the epicenter of 16.7 ºN, 99.2 ºW reported by Figueroa (1970). This is also our preferred location. Our preferred M_S is 7.7 reported by Abe and Noguchi (1983). M_w of this earthquake, estimated by Anderson *et al*. (1989), is 7.9.

26 March 1908, 23:03. Extensive damage was reported along coastal towns of Ometepec and Pinotepa Nacional, near the border of the States of Guerrero and Oaxaca.It was also felt strongly in San Marcos and Acapulco, and inland towns of Tierra Colorada, Chilapa, Tlapa, Ayutla, and Chilpancingo. There is no mention of tsunami in Acapulco. Gutenberg and Richter (1954) reported a depth of 80 km, an epicenter at 18 ºN, 99 ºW, and magnitude M of 7.8. Abe (1981) estimated m_B7.7. The depth and location, if true, suggest an intraslab earthquake. However, seismograms of this earthquake at Uppsala and Göettingen are similar to other Mexican interplate events and bear no resemblance with those of known intraslab Mexican earthquakes (e.g., 1931 Oaxaca earthquake, see Singh *et al*., 1985). We conclude that this earthquake was a shallow thrust event located SE of Acapulco. Our preferred epicenter is 16.3 ºN, 98.5 ºW. M_S and M_w, estimated from European Wiechert seismograms, are7.6 and 7.5, respectively (see Singh *et al*., 1984; Anderson *et al*., 1989).

27 March 1908, 03:45. Felt and damage reports suggest that it was an aftershock of the 26 March 1908 earthquake. It is difficult to estimate whether its epicenter was to NW or SE of the mainshock. We arbitrarily assign the same location as the mainshock: 16.3 ºN, 98.5 ºW. M_S7.0, M_w7.2.

30 July 1909, 10:51. Very strong earthquake felt in Acapulco, Chilpancingo, and Chilapa, causing damage and injuries. In Acapulco the earthquake was accompanied by sound. One report mentions that the sea retreated about 50 m. According to Muñoz Lumbier (1935), however, the sea invaded the land in Acapulco,i.e., the land subsided. As described by Muñoz Lumbier (1935), the sea had still not returned to the pre-earthquake level by 1935. If so, then it suggests that the slip on the plate interface probably did not extend farther inland than ~ 10 km from the coast. We note that during 11 May and 19 May 1962 earthquakes (M_S 6.9, 6.7) the tide gauge record in Acapulco shows an uplift of the coast. Gutenberg and Richter (1954) reported the epicenter location as

17.0 ºN, 100.5 ºW and $M_{GR} = 7^3/_4$. The epicenter listed in Figueroa (1970) is 16.8 ºN, 99.9 ºW, near Acapulco, which agree well with felt and damage reports and, hence, is our preferred location. M_S7.3, M_w7.5.

31 July 1909, 19:18. Strongly felt in Acapulco causing some damage. Reports mention that the sea receded 30 m. Most probably a large aftershock of the earthquake of the day before. The location given by Figueroa (1970) is 16.6 ºN, 99.5 ºW. We assign it the same epicenter as the earthquake of 30 Jul. 1909: 16.8 ºN, 99.9 ºW. M_S6.9, M_w7.0.

16 December 1911, 19:14. Felt strongly in Acapulco, Tecpan de Galeana and San Luis de la Loma. Epicenter listed in Gutenberg and Richter (1954) is 17.0 ºN, 100.5 ºW with M_{GR}7.5. The location given by Figueroa (1970) is 16.9 ºN, 100.7 ºW. Our preferred epicenter is 17.1 ºN, 100.7 ºW. M_S7.6, M_w7.6.

Table A1. Large, shallow earthquakes between 1899 and 1911 in the Guerrero segment of the Mexican subduction zone. A is the amplitude of ground motion in micron during 20 s surface waves at Uppsala.

Yr Mo Day	Hr	Location		Magnitude	A, Uppsala μ
		Lat.,ºN	Lon., ºW		
1899 01 24	23:43	17.1	100.5	7.5 (M_S)	-
1907 04 15	06:08	16.7	99.2	7.7 (M_S) 7.9 (M_w)	283
1908 03 26	23:03	16.3	98.5	7.6 (M_S) 7.5 (M_w)	259
1908 03 27	03:45	16.3	98.5	7.0 (M_S) 7.2 (M_w)	66
1909 07 30	10:51	16.8	99.9	7.3 (M_S) 7.5 (M_w)	120
1909 07 31	19:18	16.8	99.9	6.9 (M_S) 7.0 (M_w)	26
1911 12 16	19:14	17.1	100.7	7.6 (M_S) 7.6 (M_w)	-